




Cite this: *J. Anal. At. Spectrom.*, 2022, **37**, 2556

## Multielement analysis in soils using nitrogen microwave inductively coupled atmospheric-pressure plasma mass spectrometry†

Zengchao You,<sup>\*a</sup> Asli Akkuş,<sup>ab</sup> Wolfram Weisheit,<sup>c</sup> Thorsten Giray,<sup>a</sup> Sibylle Penk,<sup>a</sup> Sabine Buttler,<sup>a</sup> Sebastian Recknagel<sup>a</sup> and Carlos Abad <sup>\*a</sup>

In this study, we employed nitrogen microwave inductively coupled atmospheric-pressure plasma (MICAP) combined with quadrupole mass spectrometry (MS) and a liquid sample introduction system to analyze heavy metals in soils. The vanadium, cobalt, nickel, zinc, copper, chromium, arsenic, lead, and cadmium contents in seven reference and three environmental soil samples determined using MICAP-MS were within the uncertainty of the reference values, indicating that MICAP-MS is promising for soil analysis similar to the conventional inductively coupled plasma mass spectrometry (ICP-MS) technique. In addition, the limits of detection (LODs) and sensitivity of both techniques using N<sub>2</sub> and Ar plasma were of the same order of magnitude. Furthermore, the performance of MICAP-MS under different N<sub>2</sub> purity was investigated, and we found that the plasma formation and ionization efficiency were not influenced by the impurities in the gas. A prominent advantage of MICAP-MS is the low operating cost associated with gas consumption. In this work, MICAP-MS used nitrogen, which is cheaper than argon, and consumed 25% less gas than ICP-MS. Using low-purity N<sub>2</sub> can further reduce the gas cost, making MICAP-MS more cost effective than ICP-MS. These results suggest that MICAP-MS is a promising alternative to ICP-MS for the analysis of heavy metals in the soil.

Received 15th July 2022  
 Accepted 5th October 2022

DOI: 10.1039/d2ja00244b

rsc.li/jaas

Owing to the fast industrial growth and the application of metal-containing compounds, such as lithium (Li)-, cadmium (Cd)-, and lead (Pb)-based materials in batteries,<sup>1</sup> soil pollution by heavy metals has become an environmental threat.<sup>2</sup> Globally, there are already 5 million sites of soil contaminated by heavy metals.<sup>3</sup> Some heavy-metal pollutants can influence food chain safety and food quality, which, in turn, affects human health. For example, long-term exposure to arsenic (As)-contaminated food has resulted in adverse health impacts, such as stomach pain, skin lesions, and circulatory problems.<sup>4,5</sup> Pb in the soil can settle on or be absorbed by plants grown for fruits or vegetables and cannot be completely washed away. High-level lead exposure is harmful to the brain and nervous systems of vulnerable populations, such as children and fetuses.<sup>6,7</sup> Cd can accumulate in plants with a long half-life of 25–30 years. Cd exposure is also associated with various types of cancers, including breast, lung, and pancreas cancers.<sup>8,9</sup> According to the German Federal Soil Protection and Contaminated Site Ordinance (BBodSchV), 14

heavy metals in the soil, including As, Pb, and Cd, are classified as heavily toxic elements.<sup>10</sup> The adequate protection and restoration of soil requires the extensive characterization and remediation of the heavy metals.<sup>11,12</sup> Thus, elemental analysis and precise quantification of the heavy metals in soil are vital.

Inductively coupled plasma mass spectrometry (ICP-MS) is an effective technique for the trace analysis of soil owing to its multielement capability, high sensitivity, and low sample consumption.<sup>13–15</sup> However, despite its success and widespread usage, ICP-MS has several consistent drawbacks, such as high argon (Ar) gas consumption,<sup>16</sup> Ar-based polyatomic interferences,<sup>17</sup> and the need for complicated radiofrequency (RF)-power generators.<sup>18</sup> Different approaches have been employed to overcome these drawbacks; for example, low-flow plasma torches have been employed to reduce Ar gas consumption,<sup>16,19</sup> and collision and reaction cells are used to mitigate Ar-based interferences.<sup>20,21</sup>

Among these approaches, several studies have investigated the replacement of Ar plasma gas with nitrogen (N<sub>2</sub>) gas.<sup>22–24</sup> Compared to Ar, N<sub>2</sub> is inexpensive and easy to obtain. Moreover, Ar-related interferences, such as <sup>40</sup>Ar<sup>+</sup>, <sup>40</sup>Ar<sup>12</sup>C<sup>+</sup>, <sup>40</sup>Ar<sup>15</sup>N<sup>+</sup>, and <sup>40</sup>Ar<sup>16</sup>O<sup>+</sup>, which interfere with the most abundant isotopes of calcium (Ca), chromium (Cr), manganese (Mn), and iron (Fe), respectively, can be significantly reduced using N<sub>2</sub> as the plasma gas.<sup>25,26</sup> Various N<sub>2</sub>-based microwave-induced plasma

<sup>a</sup>Bundesanstalt für Materialforschung und -prüfung (BAM), Richard-Willstätter-Str. 11, D-12489 Berlin, Germany. E-mail: Zengchao.You@bam.de; Carlos.Abad@bam.de

<sup>b</sup>Berliner Hochschule für Technik (BTH), Luxemburger-Str. 10, D-13353 Berlin, Germany

<sup>c</sup>Analytik Jena GmbH, Konrad-Zuse-Str. 1, D-07745 Jena, Germany

† Electronic supplementary information (ESI) available. See DOI: <https://doi.org/10.1039/d2ja00244b>



(MIP) have been developed and used to replace the Ar-based ICP source.<sup>22,24,27</sup> In the 1990s, Hitachi coupled MIP with mass spectrometry (MS), and the instrument could be satisfactorily applied to several areas.<sup>25,28,29</sup> Thereafter, N<sub>2</sub>-based microwave inductively coupled atmospheric-pressure plasma (MICAP) was implemented with optical emission spectrometry (OES) in 2016.<sup>23</sup> This plasma exhibited good tolerance to solvent loading and different organic solvents. In 2018, MICAP was combined with time-of-flight mass spectrometry (TOFMS),<sup>18</sup> which showed slightly lower sensitivities than Ar-based ICP-MS. However, the limits of detection (LODs) for potassium (K), Ca, Cr, Fe, As, and selenium (Se), which are similar to those of most other elements, can be significantly improved. In 2021, MICAP was coupled with quadrupole mass spectrometry using laser ablation sampling (LA-(N<sub>2</sub>-MICAP)-MS) to investigate the capabilities of a high-power N<sub>2</sub> plasma with dry aerosols.<sup>30</sup> The performance of LA-(N<sub>2</sub>-MICAP)-MS was comparable to that of LA-(Ar-ICP)-MS for laser-generated aerosols.

Herein, we investigated the application of MICAP and MICAP coupled with quadrupole mass spectrometry for the elemental analysis of soil samples with the introduction of liquid samples. Seven reference and three environmental soil samples containing vanadium (V), cobalt (Co), nickel (Ni), zinc (Zn), copper (Cu), Cr, mercury (Hg), As, Pb, and Cd were digested with aqua regia and used for the analysis. The mass fractions of the selected elements were determined using MICAP-MS and validated using ICP-MS. The sensitivity, LODs, and gas consumption costs of both methods were compared and discussed in detail. Furthermore, the performance of MICAP-MS under different N<sub>2</sub> purity was investigated and compared.

## Experimental

### Sample

The reference soil samples investigated included RV24-N2 (loamy soil, grain size  $\leq 125 \mu\text{m}$ ), RV25-N2 (loamy soil, grain size  $\leq 63 \mu\text{m}$ ), RV26-N1 (loamy soil, grain size  $\leq 63 \mu\text{m}$ ), RV26-N3 (loamy soil, grain size  $\leq 63 \mu\text{m}$ ), BRM 9b (fine sandy soil, grain size  $\leq 125 \mu\text{m}$ ), BRM 10a (river sediment, grain size  $\leq 125 \mu\text{m}$ ), and BRM 13 (mixed sandy soil, grain size  $\leq 125 \mu\text{m}$ ). All reference soil samples were initially used as proficiency test samples. They were collected from Berlin, Germany, and prepared by BAM.<sup>31</sup> The mass fractions of the elements contained in the samples are listed in Table S1 (ESI<sup>†</sup>). The environmental soil sample 1 (fine sandy to mixed sandy soil, grain size  $\leq 63 \mu\text{m}$ ), sample 2 (fine sandy to mixed sandy soil, grain size 63–125  $\mu\text{m}$ ), and sample 3 (fine sandy to mixed sandy soil, grain size 125–150  $\mu\text{m}$ ) were collected from Berlin, Germany.

Calibrations were conducted with multielement solutions prepared from single-element ICP stock solutions (Merck AG, Germany). The samples were diluted using 2% nitric acid (HNO<sub>3</sub>) (Merck KGaA, Germany) in ion-exchange-cartridge-purified water (MilliQ) (Millipore, USA). The concentration of the multielement solutions ranged from 0.1 to 500  $\mu\text{g L}^{-1}$ , corresponding to the concentrations of elements in the diluted aqua regia extracts of the soil samples. <sup>6</sup>Li, <sup>45</sup>Sc, <sup>89</sup>Y, <sup>115</sup>In, <sup>159</sup>Tb, and <sup>209</sup>Bi were used as internal standards in the

calibration standards, and the concentration of the samples was 50  $\mu\text{g L}^{-1}$ .

### Soil sample preparation

The soil samples were air dried overnight and 1.5 g of each sample was added to a digestion vessel placed in a heating block (Behrotest ET2, Germany) under a reflux condenser. After moistening with 500  $\mu\text{L}$  of MilliQ water, 21 mL of concentrated hydrochloric acid (HCl) (PanReac AppliChem, USA) and 7 mL of concentrated HNO<sub>3</sub> were added stepwise to each sample. An absorption vessel filled with 10 mL 2% HNO<sub>3</sub> was placed on the reflux condenser to absorb the released nitric oxide. The reaction mixture was left to stand at room temperature for 18 h for slow oxidation. Afterward, the temperature of the heating block was progressively increased to 140 °C, and the digestion mixture was heated for 2 h at this temperature. After cooling and filtering (pore size: 0.45  $\mu\text{m}$ , GE Healthcare, UK), the solutions were diluted to 100 mL using 2% HNO<sub>3</sub> in MilliQ water and used as the stock solution. Measurements were performed on the freshly prepared 2% HNO<sub>3</sub> diluted stock solutions (100 times dilution for reference soil samples; 1000 times dilution for environmental soil samples). The humidity contents in the samples were considered. For this, 2 g of a sample was weighed and dried at 105 °C for 3 h. Each resulting dried sample was then weighed. The obtained dry masses were used for the calculations.

## Instruments

The MICAP-MS used in this work consists of a MICAP plasma source (Radom Research & Development, USA) coupled with a PlasmaQuant MS Elite quadrupole mass spectrometer (Analytik Jena GmbH, Germany). A liquid sample was introduced using a concentric pneumatic nebulizer (MicroMist, USA) combined with a cooled double pass spray chamber. The samples were transported to the nebulizer using a peristaltic pump, and the rate of liquid uptake was approximately 500  $\mu\text{L min}^{-1}$ . N<sub>2</sub> 5.0 (N<sub>2</sub> content  $\geq 99.999\%$ , Linde Gas, Germany) was used as the general nebulizer, auxiliary, and plasma gases for most MICAP-MS measurements. Furthermore, N<sub>2</sub> 2.5 (N<sub>2</sub> content  $\geq 99.5\%$ , Air Liquide, France), N<sub>2</sub> 2.8 (N<sub>2</sub> content  $\geq 99.8\%$ , Linde Gas, Germany), and N<sub>2</sub> 6.0 (N<sub>2</sub> content  $\geq 99.9999\%$ , Linde Gas, Germany) were used to investigate the performance of MICAP-MS under different nitrogen purity. Data acquisition, including mass calibration, data processing, and plots, was performed using Aspect MS software (Analytik Jena GmbH, Germany). The LODs were determined by the software according to the three-sigma rule.<sup>32</sup>

An Agilent 7500 quadrupole mass spectrometer (Agilent Technologies, USA) was used for ICP-MS. A concentric nebulizer (MicroMist, USA) was combined with a cooled double pass spray chamber and a peristaltic pump for sample introduction to keep the operating conditions as similar as possible. Ar 5.0 (Ar content  $\geq 99.999\%$ , Linde Gas, Germany) was used as the nebulizer, auxiliary, and plasma gases. Helium (He) 5.0 (He content  $\geq 99.999\%$ , Linde Gas, Germany) was used as collision



gas in the collision cell. ICP-MS MassHunter software (Agilent Technologies, USA) was used for data acquisition and processing. The operating conditions for both instruments are listed in Table 1.

## Results and discussion

### Characterization of the reference soil samples

To investigate the applicability of MICAP-MS in soil analysis, the reference soil samples, including RV24-N2, RV26-N1, BRM 9b, and BRM 10a, which contained V, Cr, Co, Ni, Cu, Zn, As, Cd, Pb, and Hg, were characterized by MICAP-MS and validated by ICP-MS. The choice of isotopes for the analysis was mainly based on the nonisobaric overlap from other elements, their abundance, and the absence of polyatomic ion interferences from the plasma. For example, the most abundant Cr isotope ( $^{52}\text{Cr}$ ) suffers polyatomic ion interference from  $^{40}\text{Ar}^{12}\text{C}^+$  in ICP-MS. Therefore,  $^{53}\text{Cr}$  was selected for the measurements for both instruments. On the other hand,  $^{60}\text{Ni}$  can interfere with Ca, forming  $^{44}\text{Ca}^{16}\text{O}^+$ ; thus,  $^{62}\text{Ni}$  was selected. Based on these

considerations,  $^{51}\text{V}$ ,  $^{53}\text{Cr}$ ,  $^{59}\text{Co}$ ,  $^{62}\text{Ni}$ ,  $^{65}\text{Cu}$ ,  $^{66}\text{Zn}$ ,  $^{75}\text{As}$ ,  $^{112}\text{Cd}$ , and  $^{207}\text{Pb}$  were selected. No significant difference was observed between matrix-adjusted calibration (2.5 mg L $^{-1}$  Ca and 0.25 mg L $^{-1}$  Mg in 2% HNO $_3$ ) and water-based calibration (2% HNO $_3$ ) for the selected elements, indicating that no significant non-spectral interferences occurred during the measurements with the high dilution factor. To guarantee reproducibility, each soil sample was digested four times independently, and the measurements for each digestion were repeated at least four times. The results obtained using both methods are the average values of the fourfold measurements.

Fig. 1 shows the percentage deviations in the mass fractions of the elements determined by ICP-MS (blue) and MICAP-MS (red) compared to their reference values (green). For most elements, the results obtained using both methods are comparable and mostly lie within the reference ranges (black). The mass fractions of V and Co in the BRM samples were not certified; therefore, they are not compared for BRM 9b and BRM 10a. Due to the smaller reference ranges, the mass fractions of several elements in the BRM samples (e.g., Cu and Pb) are slightly out of the reference ranges. Samples RV25-N2, RV26-N3, and BRM 13 showed similar results (Fig. S1–S3†).

Surprisingly, the Ni mass fractions determined by MICAP-MS differ significantly from the reference values and the ICP-MS results. Although  $^{62}\text{Ni}$  suffers polyatomic ion interference from  $^{48}\text{Ca}^{14}\text{N}^+$ , due to the low abundance of  $^{48}\text{Ca}$  (0.19% of all Ca isotopes), the effect of the interference could be negligible. Another possible interference might be  $^{48}\text{Ti}^{14}\text{N}^+$  since Ti was detected in all reference soil samples (see Table S2†), and  $^{48}\text{Ti}$  is the most abundant isotope of Ti. Moreover, the skimmer cone used in MICAP-MS is made of Ni, which can enhance the

Table 1 Operating parameters in MICAP-MS and ICP-MS

	MICAP	ICP
Plasma power	1500 W	1500 W
Nebulizer gas flow	1.25 L min $^{-1}$ N $_2$	0.85 L min $^{-1}$ Ar
Auxiliary gas flow	2.25 L min $^{-1}$ N $_2$	0.9 L min $^{-1}$ Ar
Plasma gas flow	9 L min $^{-1}$ N $_2$	15 L min $^{-1}$ Ar
Sampling depth	5 mm	9 mm
Sampling cone	Pt 1.1 mm	Pt 1.0 mm
Skimmer cone	Ni 0.5 mm	Pt 0.5 mm

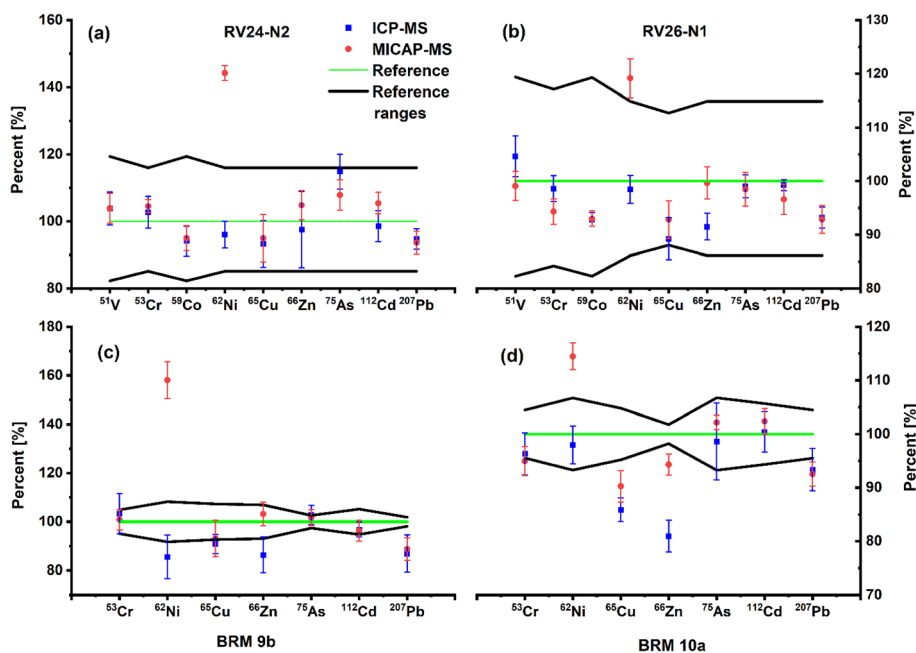


Fig. 1 Percentage deviation of the mass fractions of selected elements in soil samples (a) RV24-N2, (b) RV26-N1, (c) BRM 9b, and (d) BRM 10a determined by ICP-MS (blue) and MICAP-MS (red) compared with their reference values (green). The black lines represent the upper and lower limits of the reference ranges.



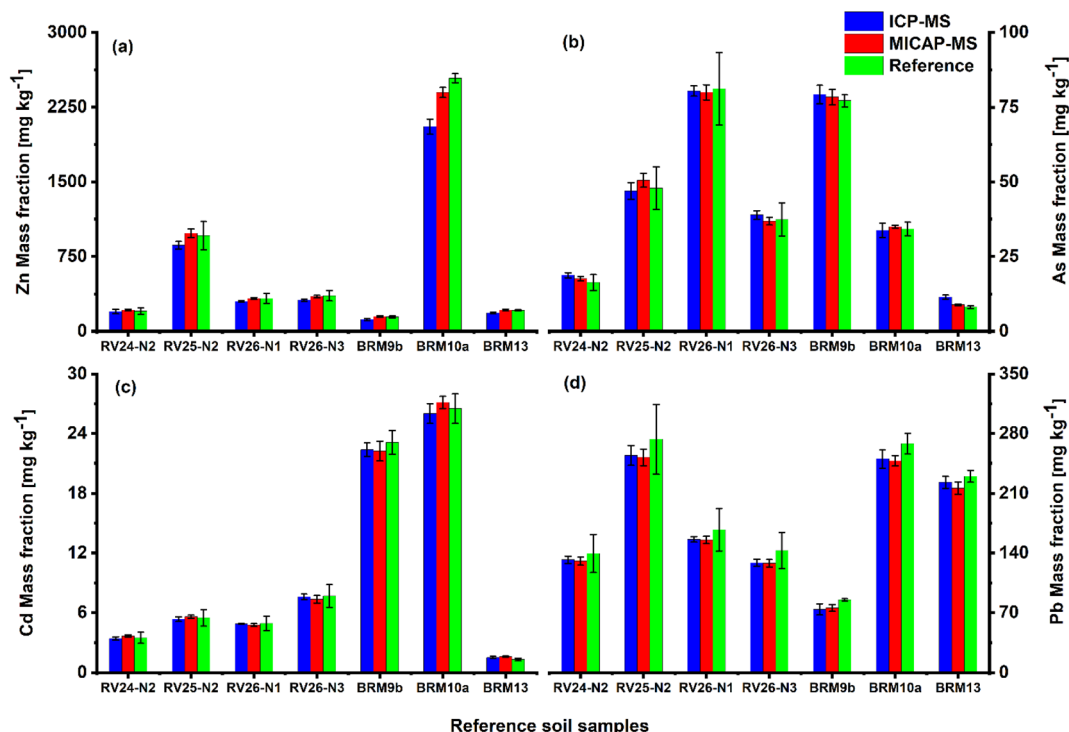


Fig. 2 Comparison of (a) Zn, (b) As, (c) Cd, and (d) Pb mass fractions in the reference soil samples determined by ICP-MS (blue) and MICAP-MS (red) with the reference values (green).

background of Ni and might also contribute to the excessive signal of Ni. The mass fractions of Zn determined by ICP-MS are lower than those determined by MICAP-MS. Although a He collision cell was employed in ICP-MS, the results could be influenced by Ar-related interferences, such as  $^{26}\text{Mg}^{40}\text{Ar}^+$ . Besides, when the soil sample with a high Ca matrix was introduced into the plasma, some plasma energy was consumed to break down the Ca matrix, which could result in the incomplete ionization of Zn since the first ionization potential of Zn (9.4 eV) is higher than that of Ca (6.1 eV). This might indicate that MICAP-MS has higher plasma energy and ionization capability than ICP-MS. However, more investigations are needed to clarify this.

Hg was also present in the reference soil samples. However, because of the strong memory effects in sample introduction systems, the Hg mass fractions determined using both methods differ greatly from the reference values and are relatively irreproducible. Therefore,  $100 \mu\text{g L}^{-1}$  of a gold (Au) solution was added to the calibration standards and samples to improve the measurement performance. Au can form a complex with Hg, presumably forming an amalgam, which, theoretically, should allow Hg to be more effectively washed out<sup>33</sup> and correspondingly enhance its signal intensity. However, no significant intensity enhancement was observed after adding Au solution. One possible reason is the low Hg concentration ( $0.1\text{--}5 \mu\text{g L}^{-1}$ ) in the diluted samples. Because of the inevitable memory effects in ICP-MS and MICAP-MS, Hg in the soil samples could not be further investigated.

As, Cd, and Pb are heavily toxic elements, which can cause serious health problems. To compare their contents, their mass fractions in all reference samples were determined using ICP-MS and MICAP-MS. The Zn mass fractions determined by ICP-MS were lower than those obtained by MICAP-MS (Fig. 1). Therefore, Zn mass fractions in all reference samples were measured for a more comprehensive analysis. Fig. 2 shows the obtained mass fractions and compares them with the reference values.

Both methods provided comparable results, which lie mostly within the reference ranges. The metrological compatibility of the obtained results with the reference values was validated using the  $E_n$  value (Tables S3–S6†), which equals the difference between the two values divided by the expanded uncertainty of this difference.<sup>34,35</sup> When  $E_n$  is less than 1, the values are considered metrologically compatible. The results of the RV samples are metrologically compatible with the reference values, whereas several values obtained for the BRM samples are not metrologically compatible due to the small reference ranges. This agrees with the results shown in Fig. 1. The Zn mass fractions in the RV25-N2, RV26-N3, and BRM13 samples determined by ICP-MS are also lower than those obtained by MICAP-MS. For As, ICP-MS showed better accuracy for RV-25-N2, RV-26-N1, and BRM 10a, whereas MICAP-MS showed better results for the other samples. For Cd and Pd, the ICP-MS results are slightly closer to the average reference values than those of MICAP-MS. Fig. S4–S7† compare the mass fractions of other elements (V, Cr, Co, and Cu) in all reference samples.



### Characterization of the environmental soil samples

To investigate the availability of the results obtained for the reference soil samples, three environmental samples were collected from Berlin, Germany. The mass fractions of the selected elements in these environmental samples were determined by ICP-MS and MICAP-MS, and the results are shown in Fig. 3.

ICP-MS and MICAP-MS showed comparable results for the environmental samples. The Zn contents determined by ICP-MS are lower than those obtained by MICAP-MS. The Ni mass fractions determined using both methods also differ significantly. For example, the Ni contents in sample 1 determined by ICP-MS and MICAP-MS are 267 and 290 mg kg<sup>-1</sup>, respectively. Thus, we conclude that, like ICP-MS, MICAP-MS is a promising method for elemental analysis and precise quantification of heavy metals in the soil.

### Comparison of LODs and sensitivities

Fig. 4(a) and Table S7† compare the LODs of both methods for the selected elements in soils. The LODs of MICAP-MS for light elements ( $m/z \leq 112$ ) were slightly higher than those of ICP-MS, which is attributed to the weaker ionization efficiency of the method due to the susceptible oxide and nitride formation in N<sub>2</sub>-based plasma.<sup>18</sup> For Ni, the LOD of MICAP-MS (337 ng L<sup>-1</sup>) was 15 times higher than that of ICP-MS (22 ng L<sup>-1</sup>), which is because the skimmer cone in MICAP-MS is made of Ni. For the heavier elements (Pb), MICAP-MS showed slightly lower LODs. The sensitivities of the methods showed a similar trend (Fig. 4(b)). For the light elements ( $m/z \leq 112$ ), ICP-MS showed higher (Co) or similar sensitivities, whereas MICAP-MS showed higher sensitivities for heavier elements, such as Pb. This could be attributed to the dissimilarities in the construction of the ion-transfer optics and different potentials applied on the instruments (see Table S8†), which could result in mass-bias of the mass analyzers in both instruments.<sup>18</sup> It could also be attributed to the stronger dependence of the ion kinetic energies on mass from the supersonic expansion of N<sub>2</sub> than Ar.<sup>36</sup>

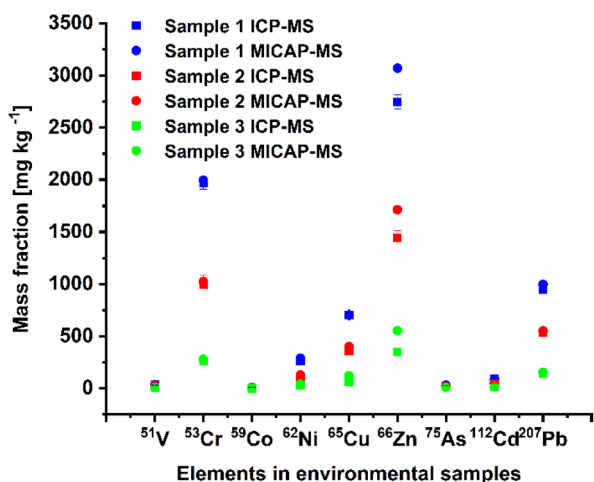


Fig. 3 Mass fractions of selected elements in the environmental soil samples determined by ICP-MS (square) and MICAP-MS (circle).

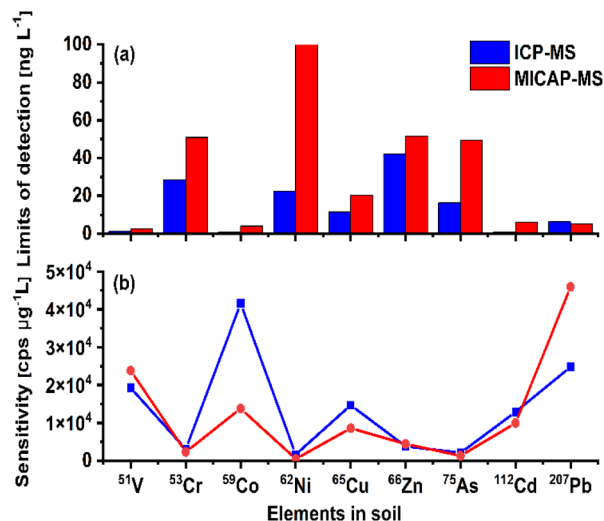


Fig. 4 Comparisons of (a) limits of detection (LODs) and (b) sensitivities of ICP-MS (blue) and MICAP-MS (red) for the selected elements in the soil samples.

### Comparison of MICAP-MS performances under different nitrogen purity

Depending on the manufacturing process, N<sub>2</sub> can be produced with different purity, which refers to the proportion of N<sub>2</sub> in the gas bottle compared to the impurities present, such as O<sub>2</sub>, H<sub>2</sub>O, Ar, CO, and CO<sub>2</sub>.<sup>37</sup> To investigate the performance of MICAP-MS under different N<sub>2</sub> purity, sample RV25-N2 was characterized using MICAP-MS under N<sub>2</sub> 2.5 (N<sub>2</sub> content  $\geq 99.5\%$ ), N<sub>2</sub> 2.8 (N<sub>2</sub> content  $\geq 99.8\%$ ), N<sub>2</sub> 5.0 (N<sub>2</sub> content  $\geq 99.999\%$ ), and N<sub>2</sub> 6.0 (N<sub>2</sub> content  $\geq 99.9999\%$ ). The mass fractions determined under different N<sub>2</sub> purity are similar (Fig. 5). For most elements, the mass fractions are almost the same. Only the results of Cr and Zn showed slight differences. This indicates that impurities in the gas do not influence the plasma formation and ionization

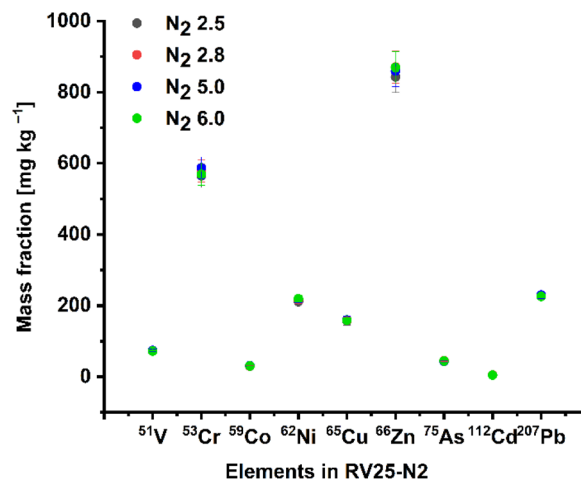


Fig. 5 Mass fractions of selected elements in RV25-N2 determined by MICAP-MS using N<sub>2</sub> with different purity grades (N<sub>2</sub> 2.5: N<sub>2</sub> content  $\geq 99.5\%$ ; N<sub>2</sub> 2.8: N<sub>2</sub> content  $\geq 99.8\%$ ; N<sub>2</sub> 5.0: N<sub>2</sub> content  $\geq 99.999\%$ ; N<sub>2</sub> 6.0: N<sub>2</sub> content  $\geq 99.9999\%$ ).



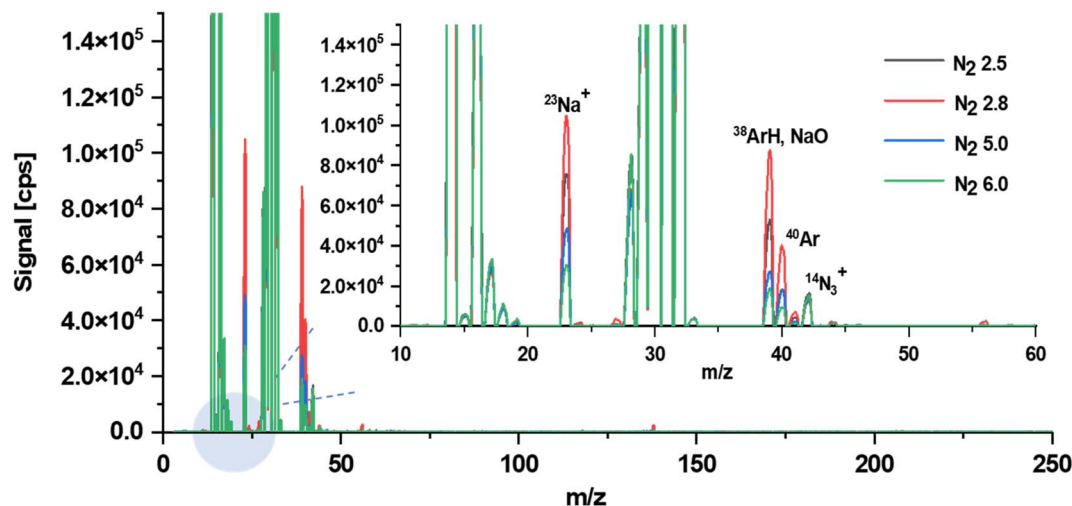


Fig. 6 Comparison of MICAP-MS mass scans for a 2%  $\text{HNO}_3$  solution obtained using  $\text{N}_2$  with different purity grades ( $\text{N}_2$  2.5:  $\text{N}_2$  content  $\geq$  99.5%;  $\text{N}_2$  2.8:  $\text{N}_2$  content  $\geq$  99.8%;  $\text{N}_2$  5.0:  $\text{N}_2$  content  $\geq$  99.999%;  $\text{N}_2$  6.0:  $\text{N}_2$  content  $\geq$  99.9999%).

efficiency of MICAP-MS; thus, they do not interfere with the selected elements in the soil.

To compare their background plasma species in MICAP-MS, the mass scans for 2%  $\text{HNO}_3$  were performed using  $\text{N}_2$  of different purities. The mass-to-charge ratios ( $m/z$ ) of the major plasma species in MICAP-MS were below 35 (Fig. 6), which corresponds to the N-related species, such as  $^{14}\text{NO}^+$ ,  $^{14}\text{N}^+$ , and  $^{14}\text{N}_2^+$ . Significant differences were observed in the results obtained using  $\text{N}_2$  with  $m/z$  of 23, 39, and 40. The species observed at  $m/z$  23 is attributed to  $^{23}\text{Na}^+$  resulting from the gas manufacturing process, and those at  $m/z$  39 and 40 are attributed to  $^{38}\text{ArH}$  and  $^{40}\text{Ar}$ , indicating that the  $\text{N}_2$  gas bottle could also contain Ar and result in Ar-related interference. This could inhibit the analysis of isotopes, such as  $^{40}\text{Ca}$ ,  $^{56}\text{Fe}$ , and  $^{75}\text{As}$ . Unexpectedly,  $\text{N}_2$  2.8 contains more impurities compared to  $\text{N}_2$  2.5. This was validated by replication measurements and could be attributed to the large quality deviation of the production process for less-pure  $\text{N}_2$  of different manufacturers (see Fig. S8 and S9<sup>†</sup>).

A remarkable advantage of MICAP-MS is the low operating cost associated with gas consumption since nitrogen is cheaper than argon. In addition, based on the calculations from the gas flow rates used in this work, MICAP-MS consumed 25% less gas than ICP-MS. The use of low-purity  $\text{N}_2$  ( $\text{N}_2$  2.5 and  $\text{N}_2$  2.8) could further reduce the gas cost of MICAP-MS, and make MICAP-MS more cost effective than ICP-MS. Furthermore, a  $\text{N}_2$  generator that can purify  $\text{N}_2$  in indoor air can be coupled with MICAP-MS, enabling the operation of MICAP-MS using indoor air; thereby, eliminating the cost of gas.

## Conclusions

We found that MICAP-MS using a liquid sample introduction is a reliable alternative to ICP-MS for the determination of heavy metals in soils. The proposed technique provided results that are comparable with ICP-MS, and consumed significantly less gas. The mass fractions of V, Co, Cu, Cr, As, Pb, and Cd in the

seven reference soil samples by MICAP-MS and ICP-MS were comparable and found mostly within the reference range. Only the results for Ni and Zn showed differences. Three environmental soil samples were collected from Berlin, Germany and used to validate the performance of both techniques. The results obtained from both techniques were comparable, proving the applicability and reliability of MICAP-MS in soil analysis.

In general, the LODs in MICAP-MS were similar or even better than ICP-MS, indicating that LODs of the same order of magnitude can be achieved using  $\text{N}_2$  and Ar plasma. We observed an exception for Ni, where the LODs in MICAP-MS were 15 times higher than ICP-MS. This was attributed to the Ni skimmer cone used in MICAP-MS. Because of the similar to LODs, the sensitivities of both techniques were considered comparable.

The performances of MICAP-MS were investigated using  $\text{N}_2$  gas with four different purity grades. The mass fractions of the elements obtained under the  $\text{N}_2$  purities were almost the same, indicating that plasma formation and ionization efficiency were not influenced by the gas impurities. Mass scans of 2%  $\text{HNO}_3$  showed that Ar may be present in the gas, which can affect the analysis of isotopes that interfere with Ar (e.g.,  $^{40}\text{Ca}$ ,  $^{56}\text{Fe}$ , and  $^{75}\text{As}$ ). In the absence of interference with the analytes, the use of low-purity  $\text{N}_2$  (e.g.,  $\text{N}_2$  2.5 and  $\text{N}_2$  2.8) could further reduce the gas cost of MICAP-MS, making MICAP-MS more cost effective than ICP-MS.

## Conflicts of interest

There are no conflicts to declare.

## Acknowledgements

The authors are grateful for the support from Analytik Jena GmbH and Radom Corp.



## References

- 1 P. Gottesfeld, F. H. Were, L. Adogame, S. Gharbi, D. San, M. M. Nota and G. Kuepou, *Environ. Res.*, 2018, **161**, 609–614.
- 2 Y. Xie, J. B. Fan, W. X. Zhu, E. Amombo, Y. H. Lou, L. Chen and J. M. Fu, *Front. Plant Sci.*, 2016, **7**, 755–760.
- 3 C. Li, K. Zhou, W. Qin, C. Tian, M. Qi, X. Yan and W. Han, *Soil Sediment Contam. Int. J.*, 2019, **28**, 380–394.
- 4 S. Anamika, *Curr. Pollut. Rep.*, 2015, **1**, 35–46.
- 5 J. O. Nriagu, P. Bhattacharya, A. B. Mukherjee, J. Bundschuh, R. Zevenhoven and R. H. Loeppert, in *Trace Metals and other Contaminants in the Environment*, Elsevier, 2007, vol. 9, pp. 3–60.
- 6 A. Kumar, A. Kumar, M. M. S. Cabral-Pinto, A. K. Chaturvedi, A. A. Shabnam, G. Subrahmanyam, R. Mondal, D. K. Gupta, S. K. Malyan, S. S. Kumar, S. A. Khan and K. K. Yadav, *Int. J. Environ. Res. Public Health*, 2020, **17**, 2179.
- 7 A.-I. Dobrescu, A. Ebenberger, J. Harlfinger, U. Griebler, I. Klerings, B. Nußbaumer-Streit, A. Chapman, L. Affengruber and G. Gartlehner, *Sci. Total Environ.*, 2022, **806**, 150480.
- 8 M. Rafati-Rahimzadeh, M. Rafati-Rahimzadeh, S. Kazemi and A. Moghadamnia, *Caspian J. Intern. Med.*, 2017, **8**, 135–145.
- 9 K. Cai, Y. Yu, M. Zhang and K. Kim, *Int. J. Environ. Res. Public Health*, 2019, **16**, 2269.
- 10 Bundes Bodenschutz- und Altlastenverordnung (BBodSchV-BGBl. I S.1328), *German Federal Ministry of Justice and Consumer Protection*, 2020.
- 11 A. Sungur, M. Soylak, E. Yilmaz, S. Yilmaz and H. Ozcan, *Soil Sediment Contam.*, 2015, **24**, 1–15.
- 12 W. Fang, Y. H. Wei and J. G. Liu, *J. Hazard. Mater.*, 2016, **310**, 1–10.
- 13 C. Moor, T. Lymberopoulou and V. J. Dietrich, *Microchim. Acta*, 2001, **136**, 123–128.
- 14 R. Falciani, E. Novaro, M. Marchesini and M. Gucciardi, *J. Anal. At. Spectrom.*, 2000, **15**, 561–565.
- 15 L. Arroyo, T. Trejos, T. Hosick, S. Machemer, J. R. Almirall and P. R. Gardinali, *Environ. Forensics*, 2010, **11**, 315–327.
- 16 P. Tirk, M. Wolfgang and H. Wiltsche, *Anal. Chem.*, 2016, **88**, 7352–7357.
- 17 S. H. Tan and G. Horlick, *Appl. Spectrosc.*, 1986, **40**, 445–460.
- 18 M. Schild, A. Gundlach-Graham, A. Menon, J. Jevtic, V. Pikelja, M. Tanner, B. Hattendorf and D. Günther, *Anal. Chem.*, 2018, **90**, 13443–13450.
- 19 A. Scheffer, R. Brandt, C. Engelhard, S. Evers, N. Jakubowski and W. Buscher, *J. Anal. At. Spectrom.*, 2006, **21**, 197–200.
- 20 P. R. D. Mason and W. J. Kraan, *J. Anal. At. Spectrom.*, 2002, **17**, 858–867.
- 21 B. Hattendorf and D. Günther, *J. Anal. At. Spectrom.*, 2000, **15**, 1125–1131.
- 22 M. R. Hammer, *Spectrochim. Acta, Part B*, 2008, **63**, 456–464.
- 23 A. J. Schwartz, Y. Cheung, J. Jevtic, V. Pikelja, A. Menon, S. J. Ray and G. M. Hieftje, *J. Anal. At. Spectrom.*, 2016, **31**, 440–449.
- 24 C. I. M. Beenakker, *Spectrochim. Acta, Part B*, 1976, **31**, 483–486.
- 25 K. Oishi, T. Okumoto, T. Iino, M. Koga, T. Shirasaki and N. Furuta, *Spectrochim. Acta, Part B*, 1994, **49**, 901–914.
- 26 T. W. May and R. H. Wiedmeyer, *At. Spectrosc.*, 1998, **19**, 150–155.
- 27 Y. Okamoto, M. Yasuda and S. Murayama, *Jpn. J. Appl. Phys.*, 1990, **29**, L670–L672.
- 28 J. Yoshinaga, T. Shirasaki, K. Oishi and M. Morita, *Anal. Chem.*, 1995, **67**, 1568–1574.
- 29 A. Chatterjee, Y. Shibata, J. Yoshinaga and M. Morita, *J. Anal. At. Spectrom.*, 1999, **14**, 1853–1859.
- 30 C. Neff, P. Becker, B. Hattendorf and D. Günther, *J. Anal. At. Spectrom.*, 2021, **36**, 1750–1757.
- 31 H. Scharf and W. Bremser, *Anal. Bioanal. Chem.*, 2015, **407**, 3219–3223.
- 32 F. Pukelsheim, *Am. Stat.*, 1994, **48**, 88–91.
- 33 E. Fatemian, J. Allibone and P. J. Walker, *Analyst*, 1999, **124**, 1233–1236.
- 34 A. Winckelmann, D. Morcillo, S. Richter, S. Recknagel, J. Riedel, J. Vogl, U. Panne and C. Abad, *Anal. Bioanal. Chem.*, 2022, **414**, 251–256.
- 35 J. Vogl, M. Rosner, S. A. Kasemann, R. Kraft, A. Meixner, J. Noordmann, S. Rabb, O. Rienitz, J. A. Schuessler, M. Tatzel and R. D. Vocke, *Geostand. Geoanal. Res.*, 2020, **44**, 439–457.
- 36 H. Niu and R. S. Houk, *Spectrochim. Acta, Part B*, 1996, **51**, 779–815.
- 37 T. Hu, H. Zhou, H. Peng and H. Jiang, *Front. Chem.*, 2018, **6**, 329–335.

